APPLIED AND ENVIRONMENTAL MICROBIOLOGY, Feb. 1995, p. 769–777 Vol. 61, No. 2
0099-2240/95/$04.00+0

Channel Structures in Aerobic Biofilms of Fixed-Film Reactors Treating Contaminated Groundwater

ARTURO A. MASSOL-DEYÁ,[1,2]† JOANNE WHALLON,[3] ROBERT F. HICKEY,[1,4] AND JAMES M. TIEDJE[1,2,3]*

Center for Microbial Ecology,[1] Department of Microbiology,[2] and Department of Crop and Soil Sciences,[3] Michigan State University, East Lansing, Michigan 48824, and Michigan Biotechnology Institute, Lansing, Michigan 48909[4]

Received 17 May 1994/Accepted 5 December 1994

Scanning electron microscopy, confocal scanning laser microscopy, and fatty acid methyl ester profiles were used to study the development, organization, and structure of aerobic multispecies biofilm communities in granular activated-carbon (GAC) fluidized-bed reactors treating petroleum-contaminated groundwaters. The sequential development of biofilm structure was studied in a laboratory reactor fed toluene-amended groundwater and colonized by the indigenous aquifer populations. During the early stages of colonization, microcolonies were observed primarily in crevices and other regions sheltered from hydraulic shear forces. Eventually, these microcolonies grew over the entire surface of the GAC. This growth led to the development of discrete discontinuous multilayer biofilm structures. Cell-free channel-like structures of variable sizes were observed to interconnect the surface film with the deep inner layers. These interconnections appeared to increase the biological surface area per unit volume ratio, which may facilitate transport of substrates into and waste products out of deep regions of the biofilm at rates greater than possible by diffusion alone. These architectural features were also observed in biofilms from four field-scale GAC reactors that were in commercial operation treating petroleum-contaminated groundwaters. These shared features suggest that formation of cell-free channel structures and their maintenance may be a general microbial strategy to deal with the problem of limiting diffusive transport in thick biofilms typical of fluidized-bed reactors.

The contamination of groundwater resources with aromatic and alkyl group-substituted aromatic hydrocarbons has become a serious threat to human health (10). Leakage from underground gasoline and petroleum storage tanks and distribution systems represents a major source of this pollution. Pump-and-treat remediation techniques have often been implemented to control contaminate plumes. Fixed-film biological systems developed on porous media have recently been employed for the treatment phase. Through either attachment or agglomeration, bacteria may remain in place within the porous medium forming biofilm communities. The granular activated-carbon (GAC) fluidized-bed reactor (FBR) couples the absorptive and high surface-area-per-unit-volume properties of activated carbon with biological treatment to obtain robust high-capacity treatment (11, 16, 26, 27). Under optimum conditions, up to 99% of the total applied organic load can be removed with 5- to 10-min hydraulic retention times.

Past structural studies of aerobic biofilms by traditional light microscopy and transmission and scanning electron microscopy show randomly distributed cells. This result has led to process models which assume generally homogeneous biofilms (8, 29). Bacterial cells living in a dense multilayer matrix, however, face the problem of limited transport of substrate and nutrients into the film inner layers as well as export of waste products out of these deep regions. The use of microsensor technology has shown the existence of steep oxygen gradients within aerobic biofilms, thus demonstrating the importance of diffusion processes in biofilm systems (9, 17, 23). Temporal and spatial stabilities of biofilm communities against disturbances or lethal factors have been demonstrated (1, 2). The resilience of such systems to environmental changes has been largely attributed to the interdependency of the community members for nutrient exchange and to the creation and maintenance of microenvironmental conditions which can be completely different from the adjacent liquid phase (3, 7).

Confocal scanning laser microscopy (CSLM) allows the detailed, nondestructive examination of thick microbial biofilms. The advantages of CSLM in studying biofilm structures were described by Caldwell et al. (4). Careful examination by CSLM of laboratory-grown biofilms has revealed the presence of specific cell distribution patterns and large internal void spaces (18, 30). In view of these findings and the importance of efficient fixed-film processes, we investigated whether there were any structural traits in FBR biofilms that might be important to biofilm functions. The specific objectives were to describe structural patterns and properties of newly colonized GAC in a laboratory reactor operated at an organic loading rate typical of full-scale reactors and to assess whether common spatial arrangement and cell distribution strategies exist regardless of carbon sources or microbial composition in commercially operating field reactors.

MATERIALS AND METHODS

GAC-FBR and support medium. A 1-liter-working-volume sterile glass column reactor (2.54-cm diameter; 195 cm long) was used in this study. The bioreactor was operated as a one-pass up-flow system without recycling at a flow rate of 0.2 liter/min. Groundwater from a deep aquifer underlying the Michigan State University campus was amended with 32 μmol of toluene per liter (3 ppm). In addition, the influent was supplemented with pure oxygen (approximately 406 μM final concentration) and a nutrient solution (NH_4Cl and KH_2PO_4) to achieve a carbon/nitrogen/phosphorus ratio of 30:5:1. About 100 g of sterile GAC (Calgon Filtrasorb 400; Calgon Company, Pittsburgh, Pa.) was added to

* Corresponding author. Mailing address: Center for Microbial Ecology, 540 Plant and Soil Science Building, Michigan State University, East Lansing, MI 48824-1325. Fax: (517) 353-2917. Electronic mail address: 21394jmt@msu.edu.

† Present address: Department of Biology, University of Puerto Rico, Mayagüez, PR 00680.

the reactor as an adsorbent and biomass carrier. The geometric mean granule diameter was approximately 0.7 mm, with an average density of 1.6. The bed height was controlled at the desired level (maximum working height of 180 cm) by inserting a brush in the column and, by gentle agitation, shearing excess biomass. The GAC particles now freed of biomass returned by gravity to the bottom of the reactor column, while the sheared biomass was carried away in the effluent stream.

In addition, we examined field-scale GAC-FBRs currently used for the treatment of groundwater contaminated with complex mixtures of hydrocarbon compounds at different sites in Michigan (Table 1). Samples were collected from biofilm-GAC communities and stored at 4°C (generally less than 24 h) until analysis was performed.

Analytical procedures. Analyses of physicochemical parameters of the toluene-fed GAC-FBR were conducted at 2- to 3-day time intervals. Analyses included toluene disappearance, oxygen consumption, temperature, and pH. For toluene determination, 5-ml samples of influent and effluent groundwater were collected in 10-ml vials. In order to stop any further biodegradation or loss of volatiles, approximately 0.10 ml of 6 N HCl was added to each liquid sample. Tubes were sealed with Teflon-coated butyl rubber septa and aluminum crimp seals and stored at 4°C. Analysis was generally performed within a week. Toluene was analyzed by using a Varian 3700 gas chromatograph equipped with an automatic headspace sampler and a flame ionization detector. Sample quantification was performed with external standards. A polarographic electrode (overflow funnel with built-in stirring bar) coupled to a digital pH and millivolt meter (Orion model 611) was used to measured dissolved oxygen (DO) concentration and pH. DO consumption is reported as the difference between the influent and effluent readings.

Microbiological procedures. Microbial cells were removed from the activated carbon (~0.2 g [wet weight]) and homogenized by repetitive vortexing (three times for 45 s) in 1 ml of cell extraction buffer. The extraction buffer contained 0.001 M EGTA (ethylene glycol-tetraacetate [Sigma]), 0.0004 M Tween 20 (Sigma), 0.01% (wt/vol) peptone, and 0.007% (wt/vol) yeast extract in phosphate buffer (28). Bacterial numbers from GAC samples were determined by acridine orange epifluorescence microscopy by the method of Zimmerman et al. (32). Biofilm homogenates (1 ml) were fixed in 10 ml of Milli Q filter-sterilized H_2O with 0.1% (vol/vol) formaldehyde (final concentration) and then stored at 4°C until processed. A Leitz microscope, equipped for epifluorescence with a filter block consisting of a BP 450–490 excitation filter, 510 dichroic mirror, and LP 515 barrier filter, was used for the observation and enumeration of microbial cells.

Microbial activity of biofilm homogenates was determined by measuring rates of degradation of toluene. Duplicate samples were incubated in basal salt medium (20) containing 109 μmol of toluene per liter. The inoculated medium (5 ml) was added to 10-ml vials, sealed with Teflon-coated butyl rubber stoppers and aluminum crimp seals. Samples were incubated at 25°C and fixed at different time intervals with approximately 0.10 ml of 6 N HCl, and then the head space was analyzed for toluene disappearance; subsamples were amended with 0.1% (vol/vol) formaldehyde for acridine orange direct cell counts.

SEM. Samples for scanning electron microscopy (SEM) were fixed with 0.1 M phosphate buffer (pH 7.0) containing 4% glutaraldehyde for 1 h, washed with 0.1 M phosphate buffer for 10 min, and then dehydrated through a graded series of ethanol solutions (25, 50, 75, and 100% ethanol). The samples were then critical point dried and coated with gold. SEM micrographs were taken with a JSM 35C SEM (JEOL, Ltd., Tokyo, Japan).

CSLM. A Zeiss 210 CSLM (Carl Zeiss Inc., Thornwood, N.Y.) was used in this study. Dark-field images, for the purpose of measuring biofilm thickness, were acquired in the laser scanning transmitted (nonconfocal) mode by using a phase 3 condenser with a 10× (nonphase) objective. All samples were stained with acridine orange (0.005% final concentration) for at least 5 min and embedded with a 0.1% agarose solution at 40°C to nearly cover the biofilm-GAC complex. Samples were examined by using the 488-nm line of a dual-line argon ion laser. For fluorescence work, an LP520 barrier filter was employed. The samples consisted of 10 to 15 biofilm-coated GAC particles freshly collected at different times from the bottom 20% of the bed height. Images were recorded on Kodak Tmax 100 film with a Matrix Multicolor computerized camera unit (Agfa Matrix, Orangeburg, N.Y.) which received signals directly from the CSLM.

Community FAME analysis. Total fatty acids of microbial communities were analyzed as previously described with the Microbial ID analytical system (MIDI, Newark, Del.) (15, 25). Duplicate samples of cells collected from fresh GAC samples (approximately 0.1 g [wet weight]) were treated as follows: (i) whole-community cell preparations were saponified at 100°C with 1 ml of methanolic NaOH (15% [wt/vol] NaOH in 50% [vol/vol] methanol), (ii) esterification of the fatty acids at 80°C with 2 ml of 3.25 N HCl in 46% (vol/vol) methanol, (iii) extraction of the fatty acid methyl esters (FAME) into 1.25 ml of 1:1 (vol/vol) methyl-*tert*-butyl ether–hexane, (iv) aqueous washing of the organic extract with 3 ml of 1.2% (wt/vol) NaOH, and (v) analysis of the washed extract by gas chromatography.

Community FAME profiles were subjected to principal-component (PC) analysis to elucidate major variation and covariation patterns. PC analysis was conducted with values from each fatty acid (percentage of total fatty acids). All multivariate calculations were performed by using SYSTAT version 5.1 (SYSTAT Inc., Evanston, Ill.). All reactors were sampled for FAME concurrent with CSLM analysis (Table 1). Reactors TOL, BTEX, and TC were also sampled two or more additional times on an approximately monthly basis.

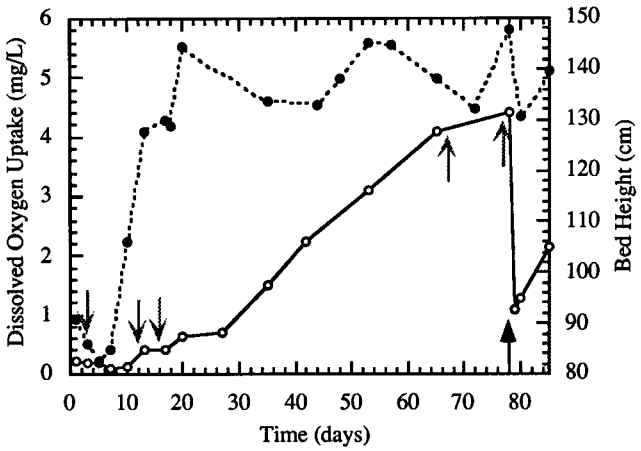

FIG. 1. Biofilm development in the toluene-fed reactor. The bed height reflects overall biofilm thickness (open circles); DO uptake is a measurement of biological activity (black circles). The stippled arrows indicate the times at which the microscopic images shown were taken. The black arrow shows the first time at which the biomass was controlled by application of shear forces.

RESULTS

Laboratory-scale GAC-FBR. The concentration of bacterial cells in the influent water fed to the toluene-amended FBR system (TOL) was approximately 10^7/liter. These microbial populations were a natural and continuous inoculum for colonization of the virgin GAC. The inlet water temperature was approximately 13°C (±1°C) throughout the experiment. The pH of the bioreactor influent and effluent was neutral.

After an initial 5- to 7-day lag phase, the DO consumption increased steadily as biomass accumulation began (Fig. 1). Steady-state conditions were assumed to have been attained when constant DO consumption occurred; this amount was also commensurate with that required for complete oxidation of the added toluene. These conditions were achieved at 15 days. The average DO consumed was 129 μmol/liter. The effluent toluene concentration was 0.72 μmol/liter for a 98% removal efficiency.

Several observations suggest that toluene biodegradation commenced once significant colonization of the GAC occurred. (i) Cell density, as observed by bed height increase (Fig. 1) and direct cell counts (data not shown), increased coincident with oxygen uptake, indicating that growth had occurred. (ii) Microbial populations capable of utilizing toluene as the sole carbon and energy source were readily isolated from the colonized GAC. (iii) On average, the specific activity of toluene oxidation by these communities was 9.9 ± 0.4 μmol/10^9 cells · day, sufficient to account for total transformation of added substrate. The initial lag phase was likely due to toluene adsorption by the GAC and the relatively cool temperature.

SEM. The surface of the GAC particles was highly irregular (Fig. 2). Close examination of the surface revealed the presence of smooth open regions, large rough zones, and open cavities. The latter two provide larger surface areas of sheltered regions and were the regions where microbial growth was initially observed (Fig. 3). After 12 days of continuous growth, the GAC surfaces were completely covered with a layer of contiguous bacterial cells embedded within a polymeric matrix (Fig. 4). The bacteria present were mainly rod shaped (0.3 to 0.6 by 1 to 3 μm), and many of them were dividing. At this

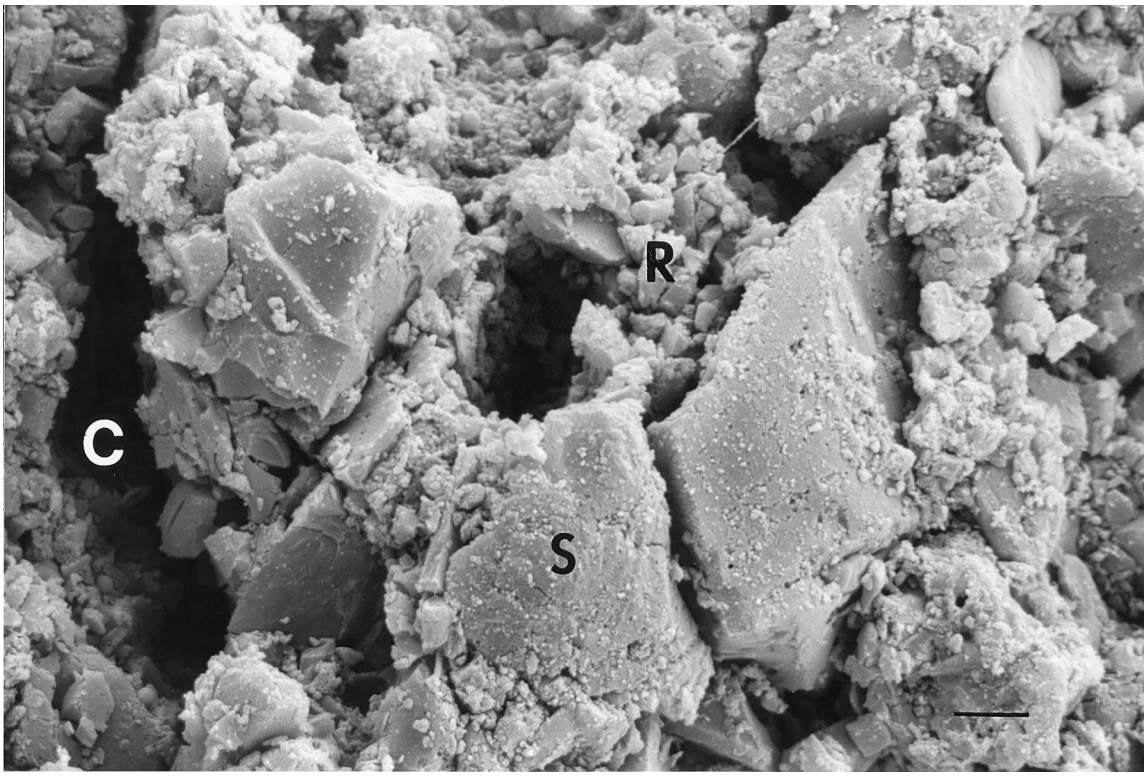

FIG. 2. SEM micrograph of sterile GAC particle showing different surface zones: smooth (S), rough (R), and cavity (C). Bar, 5 μm.

FIG. 3. SEM micrograph of a 3-day-old microcolony mainly growing over rough areas and within cavities of the GAC. Bar, 5 μm.

stage, the film depth reached 20 μm in some areas. Thicker biofilms were particularly difficult to study by SEM because the extracellular structures and bacterial cells collapsed during sample preparation.

CSLM of mature biofilms. For biofilms thicker than 15 μm, CSLM was the preferred method of studying the development of the biofilm superstructure on GAC particles. The following patterns are derived from observing 30 to 50 images from 10 to 15 granules examined at each of the sampled stages. Initially the entire surface was colonized by a thin film (10 to 20 μm) which exhibited no structural patterns (Fig. 5A). However, after the biofilm had grown much thicker (63 days), a mosaic pattern made up of separate lobes of cells was dominant (Fig. 5B). At 77 days, this lobed structure was not only maintained but even more pronounced, showing that further growth did not obliterate the channels separating the cell communities (Fig. 5C). A higher-resolution view of this stage shows that growth occurred as discrete colonial structures separated by channel boundaries (Fig. 6). These channels were typically 2 to 25 μm wide. Close examination of some of these open spaces revealed that they can extend from the top of the film to deep inner regions to form a channel-like network (Fig. 7). This overall biofilm structure was prominent after 4 to 6 weeks of operation, when biofilm function had stabilized (Fig. 1). Secondary colonizers such as yeasts and thereafter protozoa, as well as sloughing of the biomass, eventually appears to disturb the integrity of the organized biofilm structure described above. The protozoans appeared to recreate void spaces that resulted in conservation of channel-like structures by what seems to be grazing activity on bacterial cells.

Biofilms obtained from field GAC-FBRs also shared common organizational structures with the laboratory biofilms. Bacterial density ranged from 10^9 to 10^{11} cells per g of GAC in

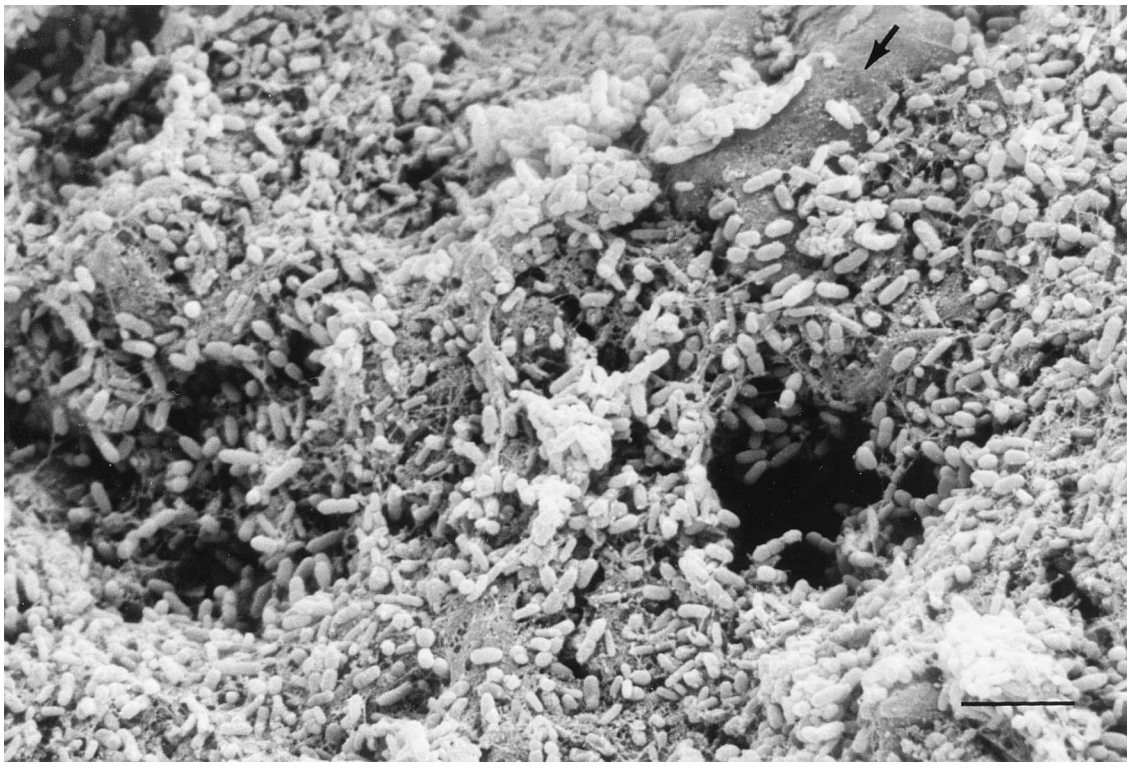

FIG. 4. SEM micrograph of a 12-day-old colonized granule from the toluene-fed reactor. Most of the surface has been colonized with actively dividing rod cells. However, there is a smooth (arrow) zone yet to be colonized. Bar, 5 μm.

all biofilm communities studied. Mature biofilms exhibited patterns in which internal contiguous cell-free spaces were commonly found in all four reactors studied (Table 1; Fig. 8). For example, the biofilm superstructure of the TC (Traverse City) field-scale FBR system exhibited contiguous void spaces opportunistically colonized by coccus-shaped cells (Fig. 8A). In contrast, the BTEX system fed benzene, toluene, ethylbenzene, and xylenes showed a coral reef-like structure, where each finger of the biofilm formed of similarly shaped cells has a particularly well-defined boundary and distribution (Fig. 8B). The dimensions of these fingers varies from 35 to 200 μm long by 20 to 40 μm thick. They all appear to develop from a contiguous base film which completely covers the GAC surface. Biofilm samples examined from two other treatment sites (PW and JEN) also displayed unique spatial cell arrangements and contiguous internal void spaces (Fig. 8C).

All thick biofilms appear to have a contiguous (e.g., TOL) or semicontiguous (e.g., TC) base layer, which was recognized by the absence of channels or other void space. In the 30-day-old biofilm sample from the Traverse City site, a discontinuous bacterial base film 10 to 25 μm deep was observed to cover the substratum from which cell-free spaces and channels appeared to develop (Fig. 9). Biofilms from the other reactor systems also showed a base film which ranged from 10 to 60 μm thick.

The vertical dimensions of the different biofilm structures were examined by laser scanning dark-field microscopy. We typically saw a high variation in biofilm thickness, even within the same colonized granule (Fig. 10), e.g., 30 to 200 μm.

Community FAME analysis of mature biofilms. Since these biofilm communities had similar structural features, we sought to evaluate how similar they might be in microbial composition by FAME analysis. The relative abundance of FAMEs from the different GAC-FBRs is presented in Table 2. A total of at least 47 fatty acids, including saturated, unsaturated, and methyl- and hydroxyl-substituted fatty acids, were identified among the samples. The greatest number and diversity of fatty acids were found for the communities in the FBR treating production water brines from an oil-producing field heavily contaminated with aromatic hydrocarbons (PW) and from the aquifer contaminated with gasoline residues (TC) at Traverse City. The most abundant fatty acids were 12:0, 14:0, 16:0, and 16:1 ω7c at these two sites. By contrast, the community with the least fatty acid diversity was the laboratory system fed only toluene (TOL), with 16:1 ω7c, 18:1 ω7c/ω9c/ω12t, and 16:0 as the dominant fatty acids. No major differences in fatty acid composition were seen in the three reactors sampled at monthly intervals (TOL, BTEX, and TC), but there were some changes in relative abundance which probably reflect shifts in population ratios.

PC analysis of FAME profiles showed that the compositions of the five GAC communities were different (Fig. 11). The first PC accounted for 41%, the second PC accounted for 25%, and the third PC accounted for 14% of the variation in the data, for a cumulative total of 80%. PC scores obtained after analysis of the correlation matrix showed high scoring (higher than 0.90) on fatty acids 13:0, a15:1, 15:0, i16:1, i16:0, 16:1 ω9c, 17:1 ω8c, 17:0, and 18:1 ω9c for PC1; 14:0, i15:0, and 16:1 ω5c for PC2; and 10:0, i14:0, and 16:0 for PC3.

DISCUSSION

Image analysis is potentially a powerful tool to aid in understanding microbial communities at an organizational level, and CSLM and other new methods are beginning to allow this potential to be realized. By using CSLM in this study of pe-

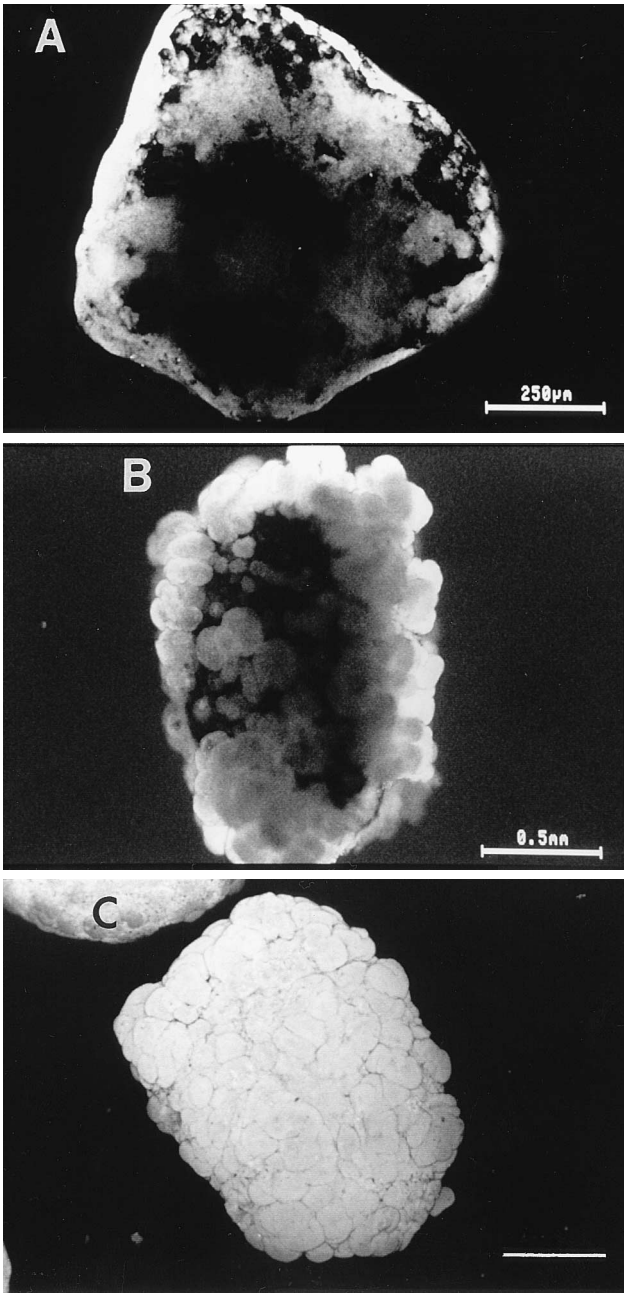

FIG. 5. Series of confocal micrographs showing biofilm growth on GAC particles in a toluene-fed reactor. Each extended focus view was constructed by computer overlay of 15 optical sections in a *z* series with a step size of 20 μm. The biofilm structure at 16 (A), 63 (B), and 77 (C) days is shown. The biofilm thickness increased from 15 to 300 μm between 16 and 77 days as determined by dark-field microscopy. Bar in panel C, 0.5 mm.

troleum-degrading films, we found that the classical model of random growth patterns leading to a uniform biofilm structure with active cells at the surface was not supported. In contrast, interaggregate channels that extend well into the biofilm appear to be maintained for long periods of time. If this model generally proves to be true, which seems to be the case in at least a few other types of biofilms examined (18, 30), then assumptions about the uniformity of diffusion within biofilms and about the location of active cells should be reevaluated.

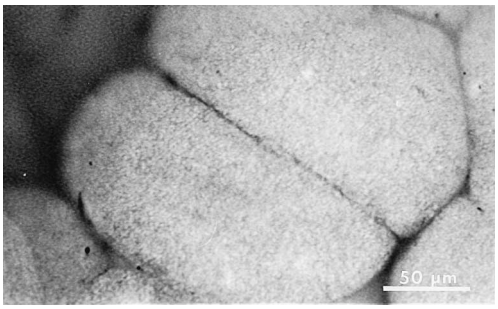

FIG. 6. Confocal micrograph of a 77-day-old biofilm showing the maintenance of colonial growth structures separated by channels in a toluene-fed reactor.

The high resolution and magnification power of SEM allowed detailed studies of the early events of preemptive surface colonization. However, sample preparation (fixation, dehydration, and embedding) introduces morphological artifacts for multilayer biofilm analysis, imposing intrinsic limitations on the film thickness which can be precisely studied. CSLM, however, allows the study of relatively thick film communities because of its ability to obtain clear optical sections free of defocus interference from underlying or overlying materials (4–6). The spatial relationships of cell arrangements, extracellular polymers, and spaces are, therefore, unaffected.

The GAC of the laboratory-scale FBR system fed ground-

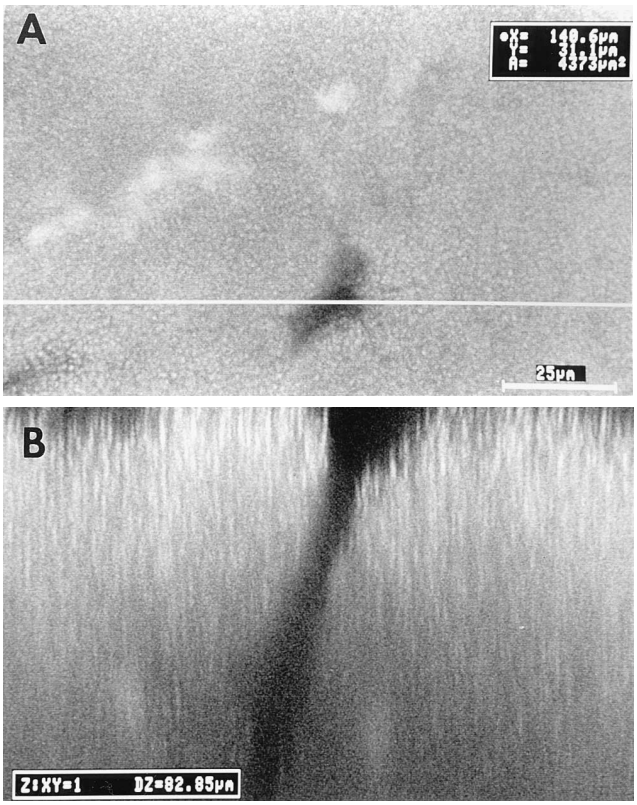

FIG. 7. Confocal micrographs of a 77-day-old biofilm showing the nature of the channel structures in the toluene-fed reactor. (A) Horizontal (*x*, *y*) optical thin section, 21 μm from the top of the biofilm (the horizontal line indicates the optical cutting position for the sagittal section). (B) Sagittal (*x*, *z*) view, showing the vertical cell distribution and the cell-free channel reaching up to the surface of the film.

TABLE 1. Description of GAC-FBRs used in this study

Bioreactor	Location[a]	Flow rate (liters/min)	Carbon source(s)	Length of operation at sampling for CSLM (mo)
TOL	MSU, East Lansing, Mich.	0.2	Toluene	6
BTEX	MBI, Lansing, Mich.	1.0	Benzene, toluene, xylenes, and ethylbenzene	1.5
TC	Traverse City, Mich.	60–80	Gasoline residues	1
PW	MBI, Lansing, Mich.	1–2	Complex mixture of aromatic hydrocarbons[b]	12
JEN	Grand Rapids, Mich.	80–100	Gasoline residues	6

[a] MSU, Michigan State University; MBI, Michigan Biotechnology Institute.
[b] This waste stream contains 7% salt.

water amended with toluene was rapidly colonized by the indigenous aquifer populations. SEM analysis showed that colonization initially occurred in sheltered regions, e.g., on rough surfaces and in cavities of the virgin GAC. This pattern of colonization is probably the result of the adsorption properties of the GAC, fluid dynamics, and system geometry. Geesey et al. (14) have shown differential bacterial colonization in the crevices of suspended detrital material in fast-moving rivers. Planar surfaces of suspended particles in FBRs are exposed to greater surface abrasion generated by shear forces and particle collisions. Eventually, however, continuous microbial growth resulted in contiguous coverage of the entire surface.

Once the particle was fully colonized, and the biofilm grew from 20 to 300 μm in thickness, we noted that a large number of vertical and horizontal channels permeated the film. These channels extended from the surfaces into at least one-half of the depth of the film. The structured, more porous film was built on a base film of 10 to 75 μm. To see if this architectural feature was the general case, especially outside of laboratory-controlled systems, we examined four field-scale FBRs treating petroleum-contaminated groundwaters. While the types of structures seen were more varied, the common feature was that channels were permeating the biofilms in all reactors.

All GAC-FBR biofilms exhibited distinctive horizontal and vertical arrangements with the following features: (i) complete GAC surface colonization and base films, (ii) irregular film edges, (iii) variable film thickness within the same colonized granule, and (iv) contiguous cell-free spaces. Open channels of variable size connected the outside film surface and bulk solution with the deeper inner layers. This biofilm structure, which increases the biological surface area per unit volume, may facilitate transport of substrates, nutrients, and gases deeper into the matrix than is possible by diffusion alone. Active bacterial cells in deep inner layers may help to keep the basal film firmly attached to the substratum and, therefore, to be more resistant against uncontrolled sloughing of the biofilm caused by shear stress or the rapid stream flow and particle collisions. Although this was not as extensively studied, late secondary colonization by yeasts, fungi, and protozoa, and mechanical biomass control (to keep the biofilm thickness from exceeding a certain depth) clearly affected the integrity of these structures in the bacterial biofilms. While we do not know the impact of these structures on biofilm performance, we do know that the reactor performance, as measured by oxygen consumption, remained constant.

It might be argued that this more porous structure is simply a result of random growth, but there are important features that suggest that this is not likely to be the entire explanation. First, the channels are maintained for many weeks, well beyond the time when confluent growth should have obliterated the channels. Second, there are a diversity of channel types which appear to be influenced by growth conditions and microbial composition. Finally, the hydraulic stress of these systems will tend to select structures which maintain their integrity, which may include mechanisms for nourishment of deeper layers in the biofilm. This more organized pattern of colonial growth suggests that some cell-to-cell communication may occur in these mixed communities.

Biofilm structure would be expected to be influenced by microbial composition. We used FAME analysis of the community to determine whether the communities of the one laboratory and four field reactors had different composition and

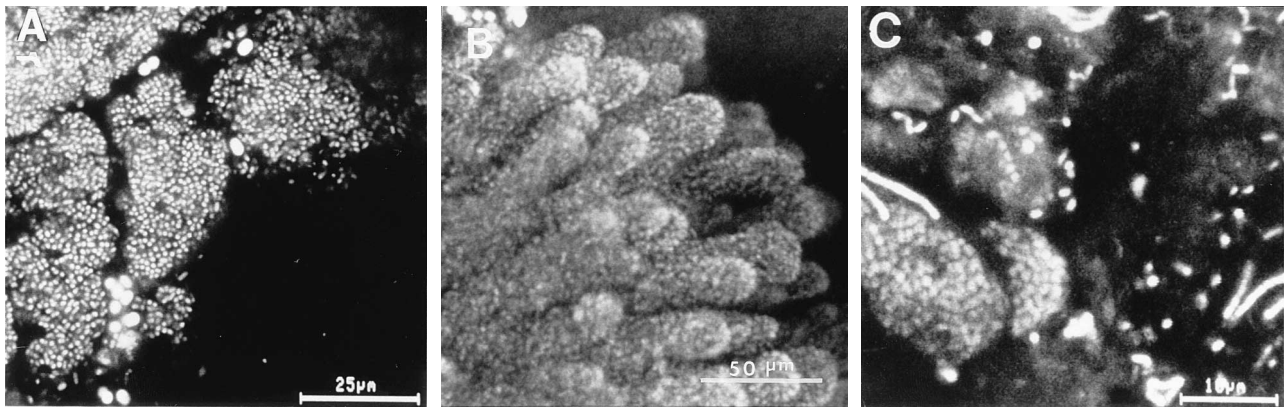

FIG. 8. Horizontal (x, y) optical sections of biofilm communities from different field-scale FBRs. Note the spacing between cell aggregates and cell arrangements. (A) TC reactor system with channel-like structure partially colonized by coccus-shaped cells. (B) BTEX system showing a coral-reef appearance of bacterial growth. (C) Biofilm structure of JEN system showing bacterial aggregates separated by well-defined void space boundaries.

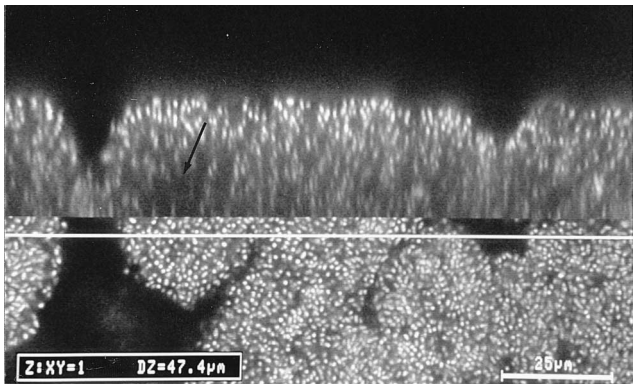

FIG. 9. Horizontal (x, y) optical section (bottom) and sagittal (x, z) optical section (top) of a 30-day-old biofilm from a field reactor site (TC) showing a fully hydrated biofilm with cell-free spaces and a discontinuous base film (arrow).

whether some were more closely related. This method has been successfully applied by several groups (12, 13, 15, 21, 22) to examine microbial community composition free of the bias inherent in culture-dependent procedures. By using PC analysis, we determined that each community had a distinct composition. The TOL (laboratory) and TC reactors were the most similar. This similarity may be due to the fact that the TOL reactor had the simplest substrate feed and, while the TC reactor had a more complex feed, it was in operation only 1 month and may not have completed its succession to a more complex community. Reactor PW was the only system that was distinguished by PC1; this reactor was the only one with a high-salt waste stream (approximately 7% [wt/vol]). In spite of the differences in microbial composition among the reactors, the channeled architecture was observed.

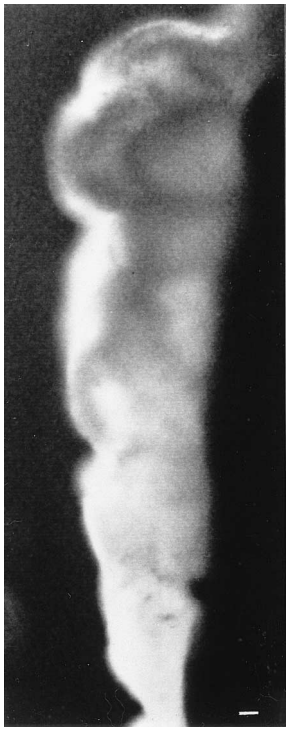

FIG. 10. Nonconfocal laser scanning dark field photomicrograph of a 77-day-old bacterial GAC-coated particle showing variation of the biofilm thickness on the same colonized surface. Bar, 15 μm.

TABLE 2. Relative abundance of fatty acids in the microbial communities of five different GAC-FBR systems

Fatty acid[a]	Relative abundance[b] (% of total) of fatty acid in reactor:				
	TOL	BTEX	TC	PW	JEN
10:0	0	6.30	0.95	1.12	1.88
i11:0	0	0	0	0	1.77
10:0 3OH	3.28	7.40	3.40	0.39	3.27
12:0	3.91	43.65	14.20	12.46	25.91
i11:0 3OH	0	0	0	0	1.68
13:0	0	0	0	0.45	0
12:0 2OH	0.75	0	0	0	0
12:0 3OH	0.91	1.07	0.14	3.32	0
i14:0	0	2.83	0	0.60	0
14:0	2.20	8.78	6.88	5.96	14.68
i15:1	0	0	1.20	0.42	0
a15:1	0	0	0	0.31	0
i15:0	0	1.93	1.03	1.80	3.44
a15:0	0	1.40	0.16	0.35	0.73
15:1 ω8c	0	0	0	0.41	0
15:1 ω6c	0	0	0.23	0.57	0
15:0	0	0	0.34	3.06	0
14:0 2OH	2.45	0	0	0	0
i14:0 3OH	0	0	0.20	0	0
16:1 ω7c alcohol	0	0	0.25	0	0
i16:1	0	0	0	1.40	0
i16:0	0	0	0	4.89	0
16:1 ω9c	0	0	0	6.33	0
16:1 ω7c	44.21	18.43	39.87	8.80	11.52
i15:0 2OH, 16:1 ω7t[c]	0	0	4.03	1.49	2.76
16:1 ω5c	0	1.65	1.00	0.15	3.41
16:0	15.60	4.61	12.46	9.49	11.70
16:0 10 methyl	0	0	0	4.74	0
i15:0 3OH	0	0	0.19	0	0
a17:0	0	0	0	0.38	0
17:1 ω8c	0	0	0.37	4.58	0
17:1 ω6c	0	0	0	1.46	0
17:0 CYCLO	0	0	0.14	0	0
17:0	0	0	0.13	1.14	0
i17:0	0	0	0.50	0.50	1.09
17:0 10 methyl	0	0	0.40	3.03	0
17:1 ω7c	0	0	0	0	0.98
16:0 3OH	0	0	0	0.28	1.33
18:3 ω6c/ω9c/ω12c[c]	0	0	0.10	0.47	0
18:1 ω9c	0	0	1.14	6.01	2.66
18:1 ω7c/ω9t/ω12t[c]	25.66	1.96	7.89	1.40	4.93
18:0	0	0	1.15	0.82	4.09
i17:0 3OH	0	0	0.22	0.09	0
19:0 CYCLO ω8c	0	0	0	0.66	0.95
20:4 ω6c/ω9c/ω12c/ ω15c[c]	0	0	0.16	0.61	0
20:0	1.03	0	0	0	0

[a] Fatty acids are designated as the number of carbon atoms, number of double bonds, and position relative to the aliphatic (ω) end of the molecule. The prefixes i and a refer to iso and anteiso branching, respectively, CYCLO indicates cyclopropane substitutions; OH indicates hydroxyl substitutions; and other methyl-branched fatty acids are designated upon the methyl group position relative to the carboxylic acid.

[b] The coefficient of variation for most fatty acids was generally below 10% for replicate analyses.

[c] A group that MIDI FAME analysis does not reliably separate.

Studies on anaerobic fixed-bed reactor communities previously revealed integrative networks of channel-like structures throughout the microbial granules which has been interpreted as playing a role in transport of cooperative substrates, nutrients, and gases (19, 24, 31). It is interesting however, that even

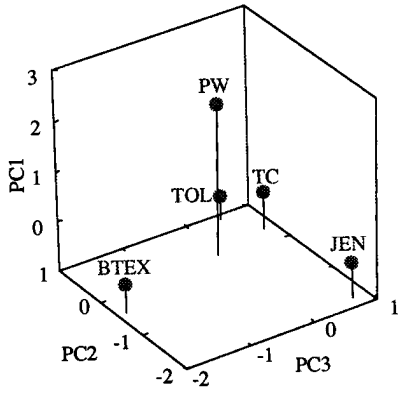

FIG. 11. PC analysis showing variation in FAME patterns in five different GAC-FBR systems: TOL, BTEX, TC, PW, and JEN.

though aerobic oxidation of hydrocarbons might require few if any interspecific interactions, microbe-microbe interactions and growth coordination seem to play a role during progressive biofilm establishment. This architecture of biofilms may represent a more optimal arrangement for the influx of substrate and nutrients and transfer of wastes and has important implications for the traditional conceptual biofilm models in which microbial growth and horizontal and vertical distribution was assumed to be randomly determined. Further testing of this model and understanding of the forces and principles which regulate biofilm development will help in efforts to model, control, and exploit biofilm-related processes of industrial, medical, and environmental importance.

ACKNOWLEDGMENTS

This work was supported by National Science Foundation grant BIR-9120006 to the Center for Microbial Ecology and by a National Institutes of Health fellowship (grant GM14047-04) to A.M.-D.

Special thanks are due to Helen Garchow for performing the FAME analysis, to the Center for Electron Optics for help with the SEM, and to Larry Forney for comments on the manuscript.

ADDENDUM

During the review of the manuscript, two important articles that provide evidence on the physiological importance of channels to biofilms appeared. deBeer et. al. (10a) showed by using oxygen microelectrodes and CSLM that O_2 concentrations were much higher in the voids than within the cell cluster and that 50% of the total O_2 consumed by the biofilm was supplied from these voids, direct evidence that the increased surface/volume ratio of channels is physiologically important. In a second article from the same group, Stoodley et. al. (26a) showed that fluorescent latex spheres 0.28 μm in diameter were mobile in channels formed by a biofilm developed by three bacterial species grown in a glucose-containing medium and that particle velocity was related to the physical structure of the biofilm. The voids or channels studied in these biofilms, however, were larger in diameter than the ones observed in our fluidized beds, which may have some influence on the physiological importance of particular channels.

REFERENCES

1. **Blenkinsopp, S. A., A. E. Khoury, and J. W. Costerton.** 1992. Electrical enhancement of biocide efficacy against *Pseudomonas aeruginosa* biofilms. Appl. Environ. Microbiol. **58:**3770–3773.
2. **Brown, M. L., and J. J. Gauthier.** 1993. Cell density and growth phase as factors in the resistance of a biofilm of *Pseudomonas aeruginosa* (ATCC 27853) to iodine. Appl. Environ. Microbiol. **59:**2320–2322.
3. **Brown, M. R. W., D. G. Allison, and P. Gilbert.** 1988. Resistance of bacterial biofilms to antibiotics: a growth-rate related effect? J. Antimicrob. Chemother. **22:**777–783.
4. **Caldwell, D. E., D. R. Korber, and J. R. Lawrence.** 1992. Confocal laser microscopy and digital image analysis in microbial ecology. Adv. Microbiol. Ecol. **12:**1–67.
5. **Carlsson, K., and A. Liljeborg.** 1989. A confocal laser microscope scanner for digital recording of optical serial sections. J. Microsc. **153:**171–180.
6. **Carlsson, K., P. Wallén, and L. Brodin.** 1989. Three-dimensional imaging of neurons by confocal fluorescence microscopy. J. Microsc. **155:**15–26.
7. **Costerton, J. W., K.-J. Cheng, G. G. Geesey, T. I. Ladd, J. C. Nickel, M. Dasgupta, and T. J. Marrie.** 1987. Bacterial biofilms in nature and disease. Annu. Rev. Microbiol. **41:**435–464.
8. **Criddle, C. S., L. A. Alvarez, and P. L. McCarty.** 1991. Microbial processes in porous media, p. 639–691. *In* J. Bear and H. Y. Corapcioglu (ed.), Transport processes in porous media. Kluwer Academic Publishers, Dordrecht, The Netherlands.
9. **Dalsgaard, T., and N. P. Revsbech.** 1992. Regulating factors of denitrification in trickling filter biofilms as measured with the oxygen/nitrous oxide microsensor. FEMS Microbiol. Ecol. **101:**151–164.
10. **Dean, J. B.** 1985. Recent findings on the genetic toxicology of benzene, toluene, xylenes and phenols. Mutat. Res. **154:**153–181.

10a. **deBeer, D., P. Stoodley, F. Roe, and Z. Lewandowski.** 1994. Effects of biofilm structures on oxygen distribution and mass transfer. Biotechnol. Bioeng. **43:**1131–1138.

11. **Ehrhardt, H. M., and H.-J. Rehm.** 1989. Semicontinuous degradation of phenol by *Pseudomonas putida* P8 adsorbed on activated carbon. Appl. Microbiol. Biotechnol. **30:**312–317.
12. **Federle, T. W., R. M. Ventullo, and D. C. White.** 1990. Spatial distribution of microbial biomass, activity, community structure, and the biodegradation of linear alkylbenzene sulfonate (LAS) and linear alcohol ethoxylate (LAE) in the subsurface. Microbiol. Ecol. **20:**297–313.
13. **Frostegard, A., A. Tunlid, and E. Baath.** 1993. Phospholipid fatty acid composition, biomass, and activity of microbial communities from two soil types experimentally exposed to different heavy metals. Appl. Environ. Microbiol. **59:**3605–3617.
14. **Geesey, G. G., and J. W. Costerton.** 1979. Microbiology of a northern river: bacterial distribution and relationship to suspended sediment and organic carbon. Can. J. Microbiol. **25:**1058–1062.
15. **Haack, S. K., H. Garchow, D. A. Odelson, L. J. Forney, and M. J. Klug.** 1994. Accuracy, reproducibility, and interpretation of fatty acid methyl ester profiles of model bacterial communities. Appl. Environ. Microbiol. **60:**2483–2493.
16. **Hickey, R. F., D. Wagner, and G. Mazewski.** 1991. Treating contaminated groundwater using a fluidized-bed reactor. Remediation **1:**447–459.
17. **Kühl, M., and B. B. Jørgensen.** 1992. Microsensor measurements of sulfate reduction and sulfide oxidation in compact microbial communities of aerobic biofilms. Appl. Environ. Microbiol. **58:**1164–1174.
18. **Lawrence, J. R., D. R. Korber, B. D. Hoyle, J. W. Costerton, and D. E. Caldwell.** 1991. Optical sectioning of microbial biofilms. J. Bacteriol. **173:**6558–6567.
19. **MacLeod, F. A., S. R. Giot, and J. W. Costerton.** 1990. Layered structure of bacterial aggregates produced in an upflow anaerobic sludge bed and filter reactor. Appl. Environ. Microbiol. **56:**1598–1607.
20. **Owens, J. D., and R. M. Keddie.** 1969. The nitrogen nutrition of soil and herbage coryneform bacteria. J. Appl. Bacteriol. **32:**338–347.
21. **Peltonen, R., W.-H. Ling, O. Hänninen, and E. Eerola.** 1992. An uncooked vegan diet shifts the profile of human fecal microflora: computerized analysis of direct stool sample gas-liquid chromatography profiles of bacterial cellular fatty acids. Appl. Environ. Microbiol. **58:**3660–3666.
22. **Rajendran, N., O. Matsuda, N. Imamura, and Y. Urushigawa.** 1992. Variation in microbial biomass and community structure in sediments of eutrophic bays as determined by phospholipid ester-linked fatty acids. Appl. Environ. Microbiol. **58:**562–571.
23. **Ramsing, N. B., M. Kühl, and B. B. Jørgensen.** 1993. Distribution of sulfate-reducing bacteria, O_2, and H_2S in photosynthetic biofilms determined by oligonucleotide probes and microelectrodes. Appl. Environ. Microbiol. **59:**3840–3849.
24. **Robinson, R. W., D. E. Akin, R. A. Nordstedt, M. V. Thomas, and H. C. Aldrich.** 1984. Light and electron microscopic examination of methane-producing biofilms from anaerobic fixed-bed reactors. Appl. Environ. Microbiol. **48:**127–136.
25. **Sasser, M.** 1990. Technical note 102: tracking a strain using the Microbial Identification System. MIDI, Inc., Newark, Del.
26. **Speitel, G. E., C.-J. Lu, M. Turakhia, and X.-J. Zhu.** 1989. Biodegradation of trace concentrations of substituted phenols in granular activated carbon columns. Environ. Sci. Technol. **23:**68–74.

26a. **Stoodley, P., D. deBeer, and Z. Lewandowski.** 1994. Liquid flow in biofilm systems. Appl. Environ. Microbiol. **60:**2711–2716.

27. **Voice, T. C., X. Zhao, J. Shi, and R. F. Hickey.** 1992. Biological activated carbon in fluidized bed reactors for the treatment of groundwater contaminated with volatile aromatic hydrocarbons. Water Res. **26:**1384–1401.

28. **Warren, T. M., V. Williams, and M. Fletcher.** 1992. Influence of solid surface, adhesive ability, and inoculum size on bacterial colonization in microcosm studies. Appl. Environ. Microbiol. **58:**2954–2959.
29. **Williamson, K., and P. L. McCarty.** 1976. A model of substrate utilization by bacterial films. J. Water Pollut. Control Fed. **48:**9–24.
30. **Wolfaardt, G. M., J. R. Lawrence, R. D. Robarts, S. J. Caldwell, and D. E. Caldwell.** 1994. Multicellular organization in a degradative biofilm community. Appl. Environ. Microbiol. **60:**434–446.
31. **Wu, W. M., R. F. Hickey, and J. G. Zeikus.** 1991. Characterization of metabolic performance of methanogenic granules treating brewery wastewater: role of sulfate-reducing bacteria. Appl. Environ. Microbiol. **57:**3438–3449.
32. **Zimmerman, R., R. Iturriaga, and J. Becker.** 1978. Simultaneous determination of the total number of aquatic bacteria and the number thereof involved in respiration. Appl. Environ. Microbiol. **36:**926–935.